

Oligomycin-induced Bioenergetic Adaptation in Cancer Cells with Heterogeneous Bioenergetic Organization

Received for publication, November 12, 2009, and in revised form, January 21, 2010. Published, JBC Papers in Press, January 28, 2010, DOI 10.1074/jbc.M109.084194

Wenshan Hao¹, Chao-Pei Betty Chang, Cheng-Chung Tsao, and Jun Xu

From the Department of Oncology, Wyeth Research, Pearl River, New York 10965

Cancer cells constantly adapt to oxidative phosphorylation (OXPHOS) suppression resulting from hypoxia or mitochondrial defects. Under the OXPHOS suppression, AMP-activated protein kinase (AMPK) regulates global metabolism adjustments, but its activation has been found to be transient. Whether cells can maintain cellular ATP homeostasis and survive beyond the transient AMPK activation is not known. Here, we study the bioenergetic adaptation to the OXPHOS inhibitor oligomycin in a group of cancer cells. We found that oligomycin at 100 ng/ml completely inhibits OXPHOS activity in 1 h and induces various levels of glycolysis gains by 6 h, from which we calculate the bioenergetic organizations of cancer cells. In glycolysis-dominant cells, oligomycin does not induce much energy stress as measured by glycolysis acceleration, ATP imbalance, AMPK activation, AMPK substrate acetyl-CoA carboxylase phosphorylation at Ser⁷⁹, and cell growth inhibition. In OXPHOS-dependent *LKB1* wild type cells, oligomycin induces 5–8% ATP drops and transient AMPK activation during the initial 1–2 h. After AMPK activation is completed, oligomycin-induced increase of acetyl-CoA carboxylase phosphorylation at Ser⁷⁹ is still detected, and cellular ATP is back at preoligomycin treatment levels by sustained elevation of glycolysis. Cell growth, however, is inhibited without an increase in cell death and alteration in cell cycle distribution. In OXPHOS-dependent *LKB1*-null cells, no AMPK activation by oligomycin is detected, yet cells still show a similar adaptation. We also demonstrate that the adaptation to oligomycin does not invoke activation of hypoxia-induced factor. Our data suggest that cancer cells may grow and survive persistent OXPHOS suppression through an as yet unidentified regulatory mechanism.

The bioenergetic organization, the fraction of cellular ATP produced by glycolysis and mitochondrial OXPHOS,² determines the bioenergetic homeostasis in cells. Tumors have a bioenergetic organization distinct from that of normal cells, in which the burden of ATP production increasingly shifts from OXPHOS to glycolysis, the so-called Warburg effect (1). Deregulation of multiple oncogenes and tumor suppressors during tumorigenesis contributes to this distinct neoplastic metabo-

lism alteration because glycolysis is the downstream target of the altered pathways (2, 3). In addition, mitochondrial defects can also drive up the aerobic glycolysis to bioenergetically compensate for the loss of OXPHOS ATP production. The reduction in OXPHOS activity has been identified in widely spread cancer cells (4–9). The switch of bioenergetic dependence from OXPHOS to glycolysis is proposed for cancer cells to cope with intermittent and chronic hypoxia microenvironments, reduce mitochondrial-initiated cell death (3, 10), and promote invasion and metastasis (10–12).

Suppression of OXPHOS activity activates master energy stress sensor AMPK that reprograms the global cellular metabolism for the stress adaptation (13, 14). In compensating for the loss of OXPHOS ATP production, activated AMPK stimulates glycolysis by coordinately promoting glucose uptake (15, 16) and glycolysis flux (17–19). AMPK-dependent activation of 6-phosphofructo-2-kinase has been demonstrated as one of the important mechanisms in stimulating glycolysis to meet cell energy needs. For example, astrocytes that have an intact AMPK/6-phosphofructo-2-kinase pathway can maintain subdued cellular ATP levels during nitric oxide-induced OXPHOS inhibition to prevent cell death, whereas neurons that lack 6-phosphofructo-2-kinase die from ATP depletion under the same condition (19, 20). In the meantime, activated AMPK phosphorylates and inactivates key enzymes in ATP-consuming anabolism to preserve ATP during energy stress (13). These include acetyl-CoA carboxylase (ACC) for fatty acid synthesis, glycerol phosphate acyl transferase for triacylglycerol synthesis, and 3-hydroxy-3-methylglutaryl-CoA reductase for cholesterol synthesis (13). Together with its effects on cell cycle and inhibition of protein synthesis, AMPK activation suppresses cell proliferation in nonmalignant as well as tumor cells (21).

Although AMPK-regulated metabolism adjustments are considered essential for cellular adaptation to OXPHOS suppression, activation of AMPK has been shown to be transient in perfused hearts and cultured cells exposed to anaerobic conditions or OXPHOS inhibitors (17, 18). After the transient AMPK activation is over, whether cells under long term OXPHOS suppression can maintain cellular ATP, survive, and grow is not known. In fact, it is proposed that the transient AMPK activation is due to the eventual depletion of cellular ATP as the result of cell death (22). There are two scenarios that might occur following the transient AMPK activation. One is that cells will not survive beyond the transient AMPK activation. The other is that AMPK activation is limited to the acute adaptation and that cells survive through reprogrammed metabolism beyond the initial phase.

¹ To whom correspondence should be addressed: Dept. of Oncology, Wyeth Research, 401 Middletown Rd., 200/4614, Pearl River, NY 10965. Tel.: 845-602-1790; Fax: 845-602-5557; E-mail: ytwhao@yahoo.com.

² The abbreviations used are: OXPHOS, oxidative phosphorylation; AMPK, AMP-activated protein kinase; ACC, acetyl-CoA carboxylase; P-ACC, ACC phosphorylation at Ser⁷⁹; 2-DG, 2-deoxy-D-glucose; HIF, hypoxia-induced factor; AICAR, 5-aminoimidazole-4-carboxamide ribonucleoside; siRNA, small interfering RNA.

Adaptation to Oligomycin-induced OXPHOS Inhibition

Cancer cells have to constantly adapt to OXPHOS suppression resulting from hypoxia or mitochondria defects. In this paper we set up experiments to understand the details of how cancer cells respond and survive the loss of OXPHOS-generated ATP. We carefully titrate down the amount of oligomycin, the mitochondria ATPase inhibitor, and use the minimal dose that completely inhibits the oxygen consumption that is responsible for mitochondria ATP generation. Recent reports on down-regulation of the catalytic subunit of the mitochondrial H^+ -ATP synthase (β -F1-ATPase) in most human carcinomas validate oligomycin as a relevant tool to study bioenergetic adaptation to OXPHOS suppression (5, 8). We have studied the specific OXPHOS suppression-related pharmacological effects in a group of cancer cells, including glycolysis acceleration, ATP imbalance, AMPK activation, phosphorylation of AMPK substrate acetyl-CoA carboxylase at Ser⁷⁹ (P-ACC), and cell growth inhibition. We find that cancer cells grow and survive the complete OXPHOS suppression, and AMPK activation plays a limited role in the adaptation.

EXPERIMENTAL PROCEDURES

Cell Lines and Reagents—Human cancer cell lines NCI-H1299 (H1299), A549, NCI-H1975 (H1975), NCI-H1650 (H1650), NCI-H520 (H520), 786-0, NCI-H838 (H838), and U87MG were obtained from American Type Culture Collection that authenticates cell lines by short tandem repeat profiling, cell morphology monitoring, karyotyping, and isoenzyme analysis. The cells were maintained in RPMI 1640 (without glutamine) supplemented with 10% (v/v) fetal bovine serum, 2 mmol/liter glutamine, 100 units/ml penicillin G, and 100 μ g/ml streptomycin sulfate (Invitrogen) for fewer than 6 months after resuscitation. Oligomycin A ($\geq 95\%$ by high pressure liquid chromatography), 2-deoxy-glucose, and 5-aminoimidazole-4-carboxamide ribonucleoside were from Sigma. Compound C was from Calbiochem.

Oxygen Consumption Measurement—Oxygen consumption was determined in the Oxygen Biosensor System plates (BD Biosciences). The cells were harvested in the test medium, and 100 μ l was loaded in assay plates that were read from the bottom of wells at regular intervals by EnVision multilabel plate reader (model 2101; PerkinElmer Life Sciences) set at an excitation of 485 nm and emission of 605 nm. Each sample was read in triplicate, and the normalized relative fluorescence unit was calculated according to the manufacturer's instructions to represent the oxygen consumption activity.

Glucose and Lactate Measurements and Calculation of Bioenergetic Organization—Cells grown at 80% confluence in 24-well plates were washed once with fresh RPMI 1640 containing 10% dialyzed fetal bovine serum and 0.2% glucose and then incubated in 300 μ l of the fresh medium with or without 100 ng/ml oligomycin for 6 h. The culture medium was collected and analyzed by CMA600 analyzer (CMA/Microdialysis) for glucose and lactate concentrations. The cells were trypsinized and counted by hemocytometer.

To calculate the glycolysis and OXPHOS components in the bioenergetic organization, we used the following: $Lac_{(c)}$ = lactate concentration in the control medium after 6 h incubation; $Lac_{(o)}$ = lactate concentration in the medium after 6 h of incu-

bation with 100 ng/ml oligomycin; Glycolysis % = $Lac_{(o)} \times 100 / Lac_{(c)}$; and OXPHOS % = $100 - Glycolysis \%$.

ATP and Oligomycin Dose-Response Growth Measurements—Cellular ATP changes were measured by CellTiter-Glo reagent according to the instructions (Promega). To measure oligomycin dose-response curves, the cells were plated in 96-well plates at ~ 400 – 500 cells/well in 100 μ l of culture, dosed the next day, and grown for 4 additional days followed by assaying with CellTiter-Glo reagent. The dose-response curves were plotted with nonlinear regression analysis of GraphPad Prism (GraphPad Software).

Immunoblotting—Whole cell extracts were prepared in the buffer containing 50 mmol/liter Tris-HCl (pH 7.5), 150 mmol/liter NaCl, 10 mmol/liter sodium pyrophosphate, 10 mmol/liter β -glycerol-2-phosphate, 50 mmol/liter NaF, 1.5 mmol/liter sodium orthovanadate, 10% glycerol, 0.5% Nonidet P-40, protease inhibitor mixture (Thermo Scientific; catalogue number 78429), and phosphatase inhibitor cocktails (Sigma; catalogue numbers P2850 and P5726). The lysates were fractionated by 4–12% gradient SDS-PAGE. The primary antibodies used were as follows: PKM1/2 (antibody 3186), ACC (antibody 3676), phospho-ACC(Ser⁷⁹) (antibody 3661), pan-AMPK α (antibody 2603), phospho-AMPK α (Thr¹⁷²) (antibody 2535) were from Cell Signaling Technology. Hexokinase II (AB3279) and LDHA (AB1222) were from Millipore. HIF-1 α was a generous gift from Dr. Robert T. Abraham's laboratory.

Cell Cycle Analysis—Cells growing at subconfluence were analyzed for cell cycle distribution. Both floating and adherent cells were harvested and combined for cell cycle analysis. The cells were fixed by 70% ethanol, digested with 0.5 mg/ml RNase A, and stained with 50 μ g/ml propidium iodide. Cell cycle analysis was performed with FACSCalibur (BD Biosciences). The data were fitted by CellQuest Pro software (BD Biosciences).

AMPK $\alpha 1$ and $\alpha 2$ siRNA—H1299 cells were transfected with siRNAs targeting AMPK $\alpha 1$ and $\alpha 2$ or nontargeting control siRNA (Dharmacon). The ON-TARGETplus SMARTpool siRNAs targeting AMPK $\alpha 1$ (PRKAA1 L-005027-00) and $\alpha 2$ (PRKAA2 L-005361-00) and ON-TARGETplus Nontargeting Pool negative control siRNA (D-001810) were obtained from Dharmacon. To knock down both AMPK $\alpha 1$ and $\alpha 2$, 20 nM of siRNA against AMPK $\alpha 1$ and $\alpha 2$ was mixed to transfect cells with Optifect (Invitrogen). As for the control, 40 nM of nontargeting control siRNA was used.

RESULTS

Oligomycin at 100 ng/ml Completely Inhibits OXPHOS and Stimulates Various Levels of Glycolysis Gain in Cancer Cells—To mimic OXPHOS suppression, we decided to use the mitochondria ATPase inhibitor oligomycin. We have selected a group of eight cell lines to study oligomycin effects. The lines have various respiration levels and glycolysis rates. In general, lines with higher respiration levels had lower glycolysis rates. To achieve specific pharmacological effects from oligomycin, we first set out to determine a low dosage of oligomycin that completely inhibits OXPHOS activity and concurrently induces a maximum glycolysis elevation. H1299 cells have a high level of respiration among the lines and were treated with various doses of oligomycin. At 100 and 1000 ng/ml, oligomycin

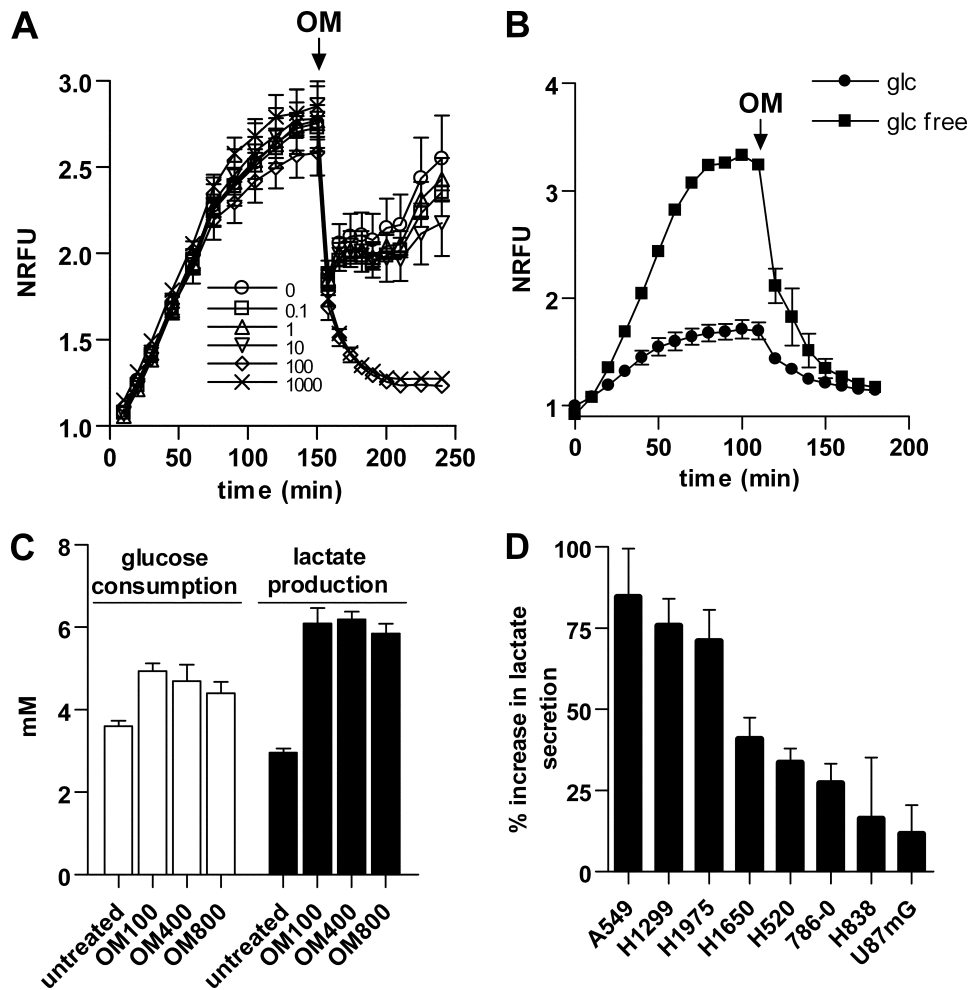


FIGURE 1. Oligomycin at 100 ng/ml inhibits OXPHOS activity and stimulates various glycolysis gains in cancer cells. *A*, respiration activity of H1299 cells was recorded for 150 min followed by adding oligomycin (OM and arrow) to 100 μ l of cells at 0.1–1000 ng/ml. Immediately, the cells were gently pipetted to mix cells with oligomycin. The pipetting led to an initial precipitous drop of fluorescent signals to all samples as the result of increased solubilization of oxygen from the atmosphere air. Bars, S.D.; $n = 3$. NRFU, normalized relative fluorescence unit. *B*, growing U87MG cells were harvested and resuspended in the medium with 10% dialyzed fetal bovine serum with or without 0.2% glucose. Respiration of cells was recorded to steady status followed by adding 100 ng/ml oligomycin (OM and arrow) to assay the kinetics of respiration inhibition. Bars, S.D.; $n = 3$. *glc*, glucose. *C*, H1299 cells were treated with 100, 400, and 800 ng/ml oligomycin for 6 h to compare the accelerating effect on glucose consumption and lactate production. Bars, S.D.; $n = 3$. *D*, cancer cells were treated with 100 ng/ml oligomycin for 6 h of treatment, and the increase in lactate secretion was measured. Bars, S.E.; $n = 3$ –5.

completely suppressed cell respiration in approximately an hour (Fig. 1A). Consistently, pretreatment of H1299 cells with 100 and 1000 ng/ml oligomycin for 60 min could completely eliminate the respiration measurement. Similar results were obtained with H1975 and A549 cells that have relatively high respiration levels (data not shown). For U87MG, 786-0, and H838 cells that have lower levels of respiration, we suspended cells in glucose-free medium to acutely stimulate respiration to higher levels. In these cells, 100 ng/ml oligomycin also completely inhibited the respiration in an hour (Fig. 1B and data not shown). As a consequence of respiration suppression, H1299 cells treated with 100 ng/ml oligomycin for 6 h accelerated glycolytic flux as indicated by higher glucose consumption and lactate production (Fig. 1C). The glycolytic flux was not further increased by raising oligomycin to 400 and 800 ng/ml (Fig. 1C), determining that 100 ng/ml oligomycin is the desired dosage for induction of OXPHOS suppression.

treated with 100 ng/ml oligomycin maintained cellular ATP after 6 h (Fig. 2C), suggesting that the increased glycolysis produces an equivalent amount of ATP to replace the loss of OXPHOS ATP. The recovery of cellular ATP levels suggested that the gains in oligomycin-induced glycolysis originated from the different contribution by OXPHOS to cellular bioenergetics prior to the oligomycin challenge. We therefore could calculate the bioenergetic organization of glycolysis and OXPHOS in cancer cells (Fig. 2D) from the oligomycin-induced glycolysis gains (Fig. 1C). The bioenergetic organizations are heterogeneous and predict differential bioenergetic dependence on glycolysis and OXPHOS for individual lines. The cells that are primarily dependent on glycolysis for ATP generation, such as 786-0, will be much less affected by oligomycin treatment. The temporary drop of ATP in H1299 but not in 786-0 cells provided a line of evidence supporting this prediction.

Applying the treatment regimen of 100 ng/ml oligomycin for 6 h to multiple cancer cell lines, we found that the glycolysis rates were accelerated in all cell lines but to various extents as indicated by the various percentage gains of lactate secretion into the culture medium (Fig. 1D). In general, cell lines with higher respiration levels show larger gains in glycolysis flux upon oligomycin treatment, indicating a greater compensatory role for glycolysis in these lines.

Oligomycin-induced OXPHOS Suppression on Cellular ATP Levels—Next we investigated how cellular ATP in this group of cancer cells changed, while cells were experiencing an oligomycin-induced inhibition of OXPHOS activity and stimulating compensatory glycolysis. H1299 and 786-0 cells, which had high and low oligomycin-induced glycolysis gains, respectively, were treated with 100 ng/ml oligomycin or 10 mM 2-deoxy-glucose (2-DG), a glycolysis pathway inhibitor. Detailed measurements of ATP levels at various time points revealed that there were statistically significant 5–8% ATP drops during the first 2 h of oligomycin treatment in H1299 cells (Fig. 2A) but not in 786-0 cells (Fig. 2B). ATP levels were fully rebalanced by 4 h of oligomycin treatment in H1299 cells (Fig. 2A). In the meantime, 2-DG led to ATP drops in both lines throughout the treatment (Fig. 2, A and B). All of the cell lines

Adaptation to Oligomycin-induced OXPHOS Inhibition

Oligomycin Induces Transient AMPK Activation but Persistent P-ACC Inductions in OXPHOS-dependent H1299 Cells—With the optimal oligomycin treatment defined, we then exam-

ined AMPK activation in oligomycin-treated cancer cells. Energy stress activates AMPK by inducing Thr¹⁷² phosphorylation (P-AMPK), which inactivates the downstream target ACC by phosphorylating it at Ser⁷⁹ (P-ACC) (13). P-AMPK in H1299 cells was stimulated after 15 min of oligomycin treatment and returned to basal levels after 1 h of treatment (Fig. 3A), indicating a transient AMPK activation in oligomycin-induced energy stress. This coincided with the time of the temporary ATP drops. The induction of P-ACC during the first hour correlated well with P-AMPK change. It peaked by 15 min and decreased by 1 h (Fig. 3A), consistent with ACC as an AMPK downstream target. However, after 1 h of treatment, the inductions of P-ACC by oligomycin could still be observed, although at a reduced levels and without AMPK activation (Fig. 3A). For further evidence that the inductions of P-ACC at 3 and 6 h of oligomycin treatment were no longer dependent on AMPK activation, we tested oligomycin effects at the presence of the pharmacological inhibitor of AMPK, Compound C (23). The inhibitor was added either with oli-

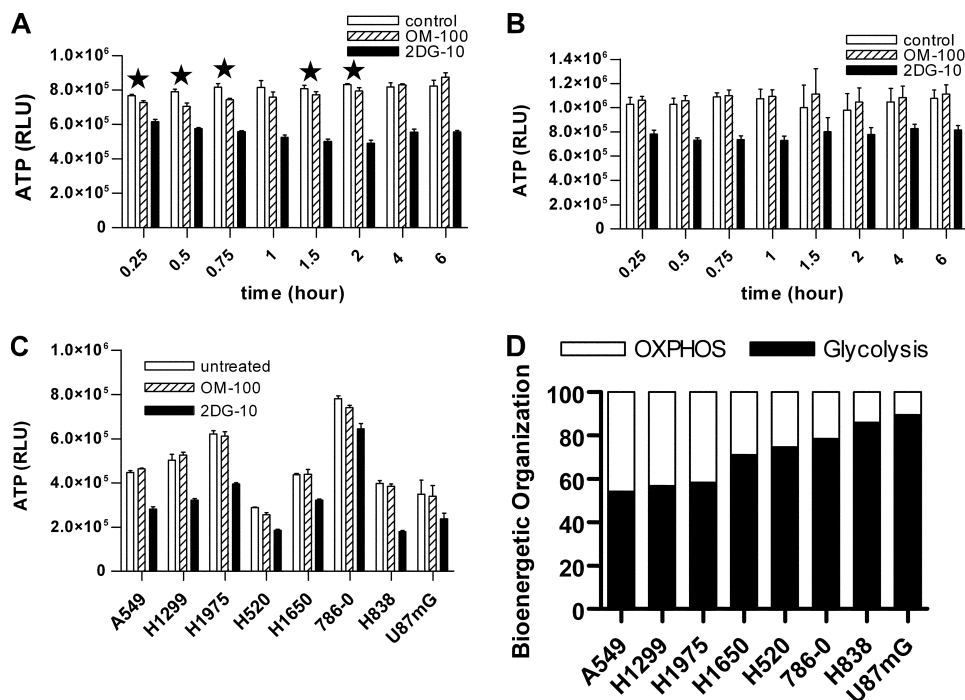


FIGURE 2. Oligomycin treatment on cellular ATP levels. Examination of ATP levels in H1299 (A) and 786-0 (B) cells treated by 100 ng/ml oligomycin (OM-100) or 10 mmol/liter 2-deoxy-glucose (2DG-10) for various times. Bars, S.D.; $n = 4$. An asterisk indicates that the difference between control and OM-100 was statistically significant with value of $p < 0.05$ (Student's t test). C, examination of ATP levels in various cancer cells treated by 100 ng/ml oligomycin (OM-100) and 10 mmol/liter 2-deoxy-glucose (2DG-10) for 6 h. Bars, S.D.; $n = 3$. D, determination of bioenergetic organizations of cancer cells.

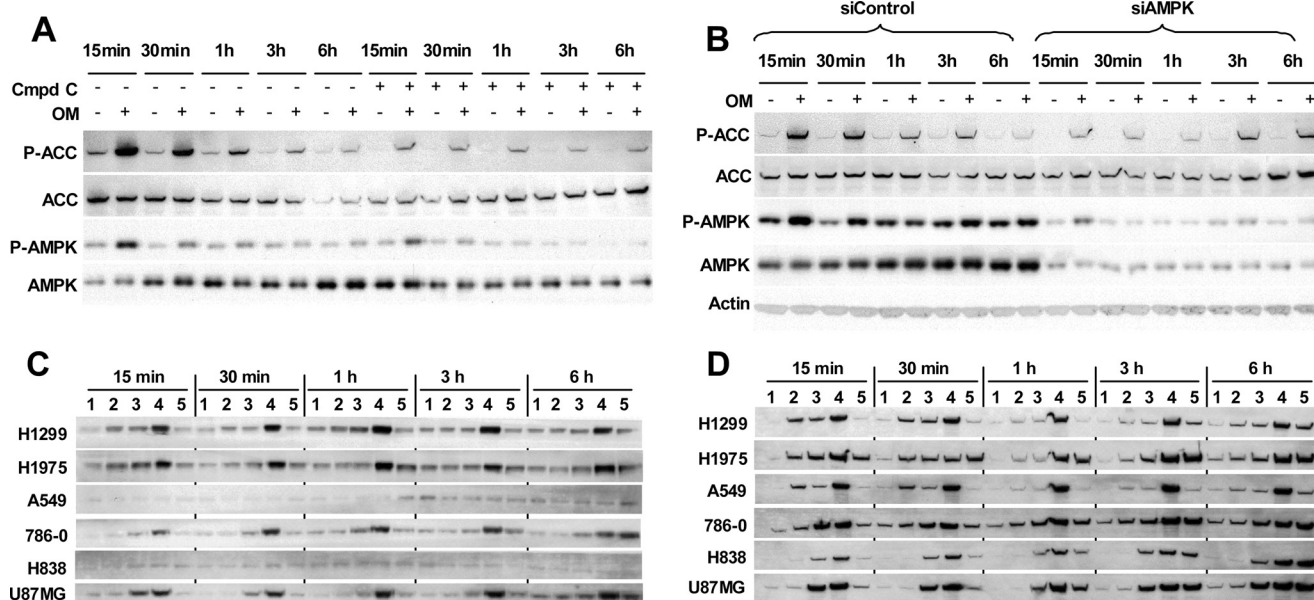


FIGURE 3. Changes of P-AMPK (Thr¹⁷²) and P-ACC (Ser⁷⁹) in cancer cells induced by energy stresses. A, H1299 cells were treated with 100 ng/ml oligomycin for various times with or without 20 μ M Compound C. For 3 and 6 h of oligomycin treatment, Compound C was added along to cells. For shorter oligomycin treatments, H1299 cells were pretreated with Compound C for 85, 70, or 40 min prior to adding 100 ng/ml oligomycin for 15, 30, and 60 min, respectively. P-AMPK and P-ACC changes were analyzed by immunoblotting. B, H1299 cells were transfected with siRNAs targeting both AMPK $\alpha 1$ and $\alpha 2$ or nontargeting control for 5 days followed by treatment with 100 ng/ml oligomycin for various times. P-AMPK and P-ACC changes were analyzed by immunoblotting. C and D, cancer cells were treated with various compounds for 15 min, 30 min, 1 h, 3 h, and 6 h. The treatments were as follows: untreated control (lanes 1); 100 ng/ml oligomycin (lanes 2); 10 mmol/liter 2-DG (lanes 3); 100 ng/ml oligomycin + 10 mmol/liter 2-DG (lanes 4); 2 mmol/liter AICAR (lanes 5). The cells were analyzed by immunoblotting for P-AMPK (Thr¹⁷²) (C) and P-ACC (Ser⁷⁹) (D) levels.

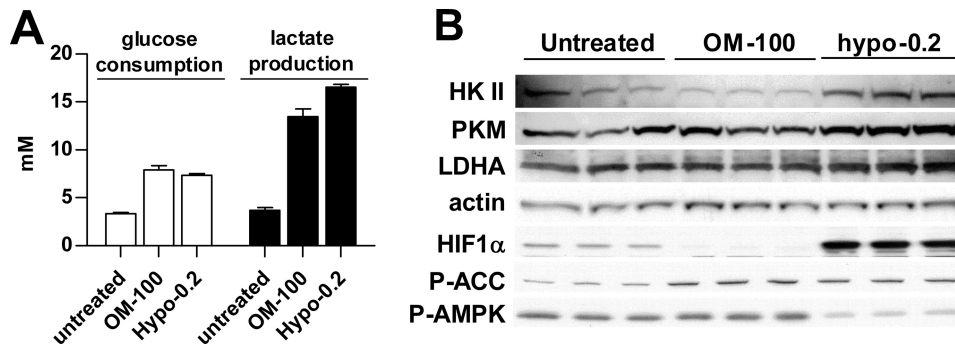


FIGURE 4. **Compare oligomycin- and hypoxia-induced glycolysis shift.** A, H1299 cells were treated with 100 ng/ml oligomycin (OM-100) and 0.2% hypoxia for 24 h. The levels of glucose and lactate in the medium were quantified and normalized by protein amount. Bars, S.D.; $n = 3$. B, expression of glycolytic enzymes and HIF1 α in cells of triplicate treatments were analyzed by immunoblotting.

gomyacin to treat cells for 3 or 6 h or to pretreat cells for 85, 70, or 40 min prior to oligomycin treatment for 15, 30, or 60 min, respectively. Compound C inhibited basal levels of P-AMPK and P-ACC, and longer exposure to the inhibitor (3 and 6 h) led to lower P-AMPK (Fig. 3A). Compound C effectively inhibited but did not completely block the transient AMPK activation. The strong inductions of P-ACC within the first hour of oligomycin treatment were effectively inhibited by Compound C. However, P-ACC inductions at 3 and 6 h were relatively much less affected, even though P-AMPK was further inhibited because of longer treatment by the inhibitor (Fig. 3A). Next, we tested the effect of AMPK inhibition by simultaneously knocking down both AMPK $\alpha 1$ and $\alpha 2$ subunits with small interference RNAs. Suppression of both basal and activated P-AMPK levels was achieved by significantly knocking down total AMPK (Fig. 3B). Under this condition, again, P-ACC inductions within first hour of oligomycin treatment were inhibited much more than inductions at 3 and 6 h (Fig. 3B). The differential impact by AMPK inhibition on P-ACC inductions was consistent with the observation that P-ACC inductions at 3 and 6 h were AMPK-independent.

P-ACC Inductions without AMPK Activation in LKB1-null Cancer Cells under Energy Stresses—LKB1 is an upstream kinase for AMPK activation, whose loss of function in cancer cells, like A549, prevents AMPK activation. We then further examined the connection of AMPK activation and P-ACC induction, induced by oligomycin, 2-DG, the combination of oligomycin and 2-DG, and the AMPK activator AICAR, in LKB1-null A549 and H838 cells versus LKB1 wild type H1299, H1975, 786-0, and U87MG cells. In wild type cells, combination of oligomycin and 2-DG induced the highest and most persistent increases in both P-AMPK and P-ACC throughout 6 h of treatment (Fig. 3, C and D, lanes 4). Similarly, AICAR triggered a gradual increase in P-AMPK over time and also corresponding P-ACC inductions (Fig. 3, C and D, lanes 5). In LKB1-null cells, consistent with the requirement of LKB1 for AMPK activation, none of the treatments activated AMPK, which remained at basal levels throughout the treatments (Fig. 3C). In contrast, high and persistent P-ACC inductions were detected in the combination treatment (Fig. 3D, lanes 4), and gradual P-ACC inductions were detected in AICAR treatment (Fig. 3D, lanes 5). Oligomycin and 2-DG alone also triggered P-ACC inductions without AMPK activation in null cells (described in

the following section). In four LKB1 wild type cells, oligomycin induced higher levels of P-AMPK in H1299 and H1975 cells than in 786-0 and U87MG cells, consistent with the prediction of bioenergetic dependence on OXPHOS by the former two cell lines. Again, we observed that oligomycin induced only transient AMPK activation (within 1 h) but persistent P-ACC inductions (3 and 6 h) in H1299 and H1975 cells (Fig. 3, C and D, lanes 2). Thus, our data suggest little involvement of AMPK activation in P-ACC induc-

tions in LKB1-null cells.

P-ACC Is a Consistent Energy Stress Marker—Bioenergetic organizations predict that A549, H1299, and H1975 cells depend on both aerobic glycolysis and OXPHOS for ATP production, whereas 786-0, H838, and U87MG cells have evolved to primarily depend on aerobic glycolysis as a power generator. Consistent with this prediction, in H1299, H1975, and A549 cells, oligomycin at 100 ng/ml or 2-DG at 10 mmol/liter stimulated similar levels of P-ACC that lasted through 6 h of treatment (Fig. 3D, lanes 2 and 3), yet in 786-0, H838, and U87MG cells, oligomycin treatment led to only a slight P-ACC increase in 786-0 cells but not much change in H838 and U87MG (Fig. 3D, lanes 2). In contrast, 2-DG induced a fast rise of P-ACC lasting through 6 h of treatment (Fig. 3D, lanes 3). Taken together, the demonstration of a tight correlation of P-ACC inductions with the intensity and duration of treatments by various energy stress inducers, independent of the status of AMPK activation, validates P-ACC as a genuine energy stress marker. The fact that the bioenergetic organizations of cancer cells accurately predict P-ACC inductions in response to glycolysis and OXPHOS inhibition confirms the functional relevance of the bioenergetic organization.

OXPHOS Suppression in Normoxia Stimulates Glycolysis without Up-regulating Key Glycolytic Enzymes—Next, we investigated whether OXPHOS suppression-induced glycolysis increases the required up-regulation of glycolytic enzymes, which accounts for hypoxia-induced glycolysis as the result of activation of HIF (24). H1299 cells were treated with 100 ng/ml oligomycin in normoxia or 0.2% hypoxia. After 24 h of treatment, hypoxia, which induced both OXPHOS inhibition and HIF activation, stimulated only 23% more lactate production than oligomycin (Fig. 4A). As expected, hypoxia activated HIF-1 α and up-regulated key glycolytic enzymes hexokinase II, pyruvate kinase M, and lactate dehydrogenase A (Fig. 4B). In contrast, oligomycin even slightly lowered HIF-1 α levels without changing glycolytic enzymes (Fig. 4B). After 24 h of treatment, oligomycin-induced P-ACC was detected without noticeable P-AMPK increase (Fig. 4B), further supporting the view that the elevation of P-ACC is a better indicator of energy stress. Interestingly, in hypoxia-treated cells, P-ACC was observed even with lowered P-AMPK (Fig. 4B). The ratio of consumed glucose over the produced lactate was ~ 2 for hypoxia treatment and smaller for oligomycin treatment

Adaptation to Oligomycin-induced OXPHOS Inhibition

(Table 1), indicating a complete glycolytic degradation of one glucose to two pyruvates and lactates in hypoxia but not with oligomycin treatment.

Cancer Cells under Long Term OXPHOS Suppression Survive on Glycolysis ATP but Endure Specific OXPHOS Inhibition-dependent Growth Slowdown—With AMPK activation limited to the initial oligomycin-induced energy stress, we further evaluated whether cancer cells can grow and survive in the long run without significant AMPK involvement in rebalancing cellular ATP. H1299 and H1650 cells, which had the bioenergetic organizations of 57 glycolysis/43 OXPHOS and 71 glycolysis/29 OXPHOS, respectively, were treated with 100 ng/ml oligomycin for 5 days. H1299 cells roughly doubled daily and grew from 10,000 to ~350,000 cells (Fig. 5A). In contrast, H1299 cells treated with oligomycin doubled their doubling time and grew from 10,000 to only 50,000 cells (Fig. 5A). Therefore, 5-day

oligomycin treatment led to ~86% growth inhibition. The slower growth was not due to the faster exhaustion of medium nutrients or accumulation of more lactate in the medium resulting from the accelerated glycolysis flux, because the daily medium change on oligomycin-treated cells did not improve the growth rate (Fig. 5A). Monitoring the changes of metabolites in cell culture medium revealed that the slowly growing oligomycin-treated H1299 cells consumed glucose and produced lactate similar to the amounts by untreated cells (Fig. 5B), suggesting an ~86% increase in cellular glycolysis rate in oligomycin-treated cells, similar to the increase measured at 6 h of treatment (Fig. 1D). Consistently, the cells treated with oligomycin for 5 days did not have altered cellular ATP levels (data not shown). Thus, oligomycin treatment forced H1299 to adopt a completely glycolytic growth at a much slower rate.

H1299 cells cultured with oligomycin did not show noticeable morphological changes nor produce more floating cells by microscopic observation (data not shown). Cell cycle analysis indicated that the slowly growing H1299 cells had a negligible increase in cells at the sub-G₁ phase, a slight increase at the G₁ phase, and a slight decrease at both the S and G₂/M phases (Fig. 5C). Therefore, complete suppression of OXPHOS in cancer cells did not inflict any detrimental consequences and arrest cells at a particular phase.

TABLE 1

The ratio of lactate produced over glucose consumed by H1299 cells treated with 100 ng/ml oligomycin (OM-100) or 0.2% hypoxia for various times

	3 h	6 h	24 h
Control	0.7	0.7	1.1
OM-100	1.1	1.2	1.7
Hypoxia	2.0	2.2	2.3

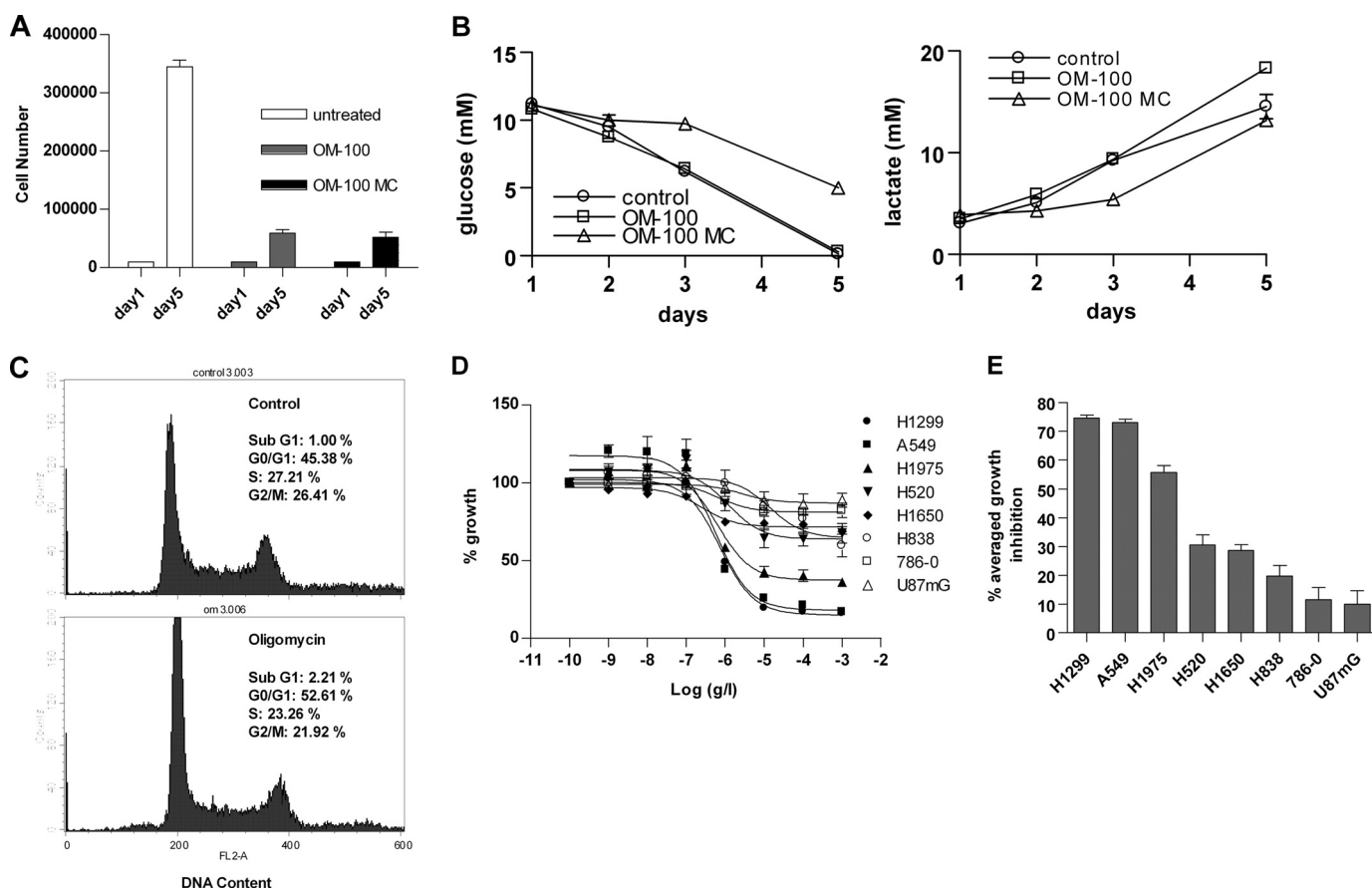


FIGURE 5. Long term oligomycin effect on cancer cells. A, H1299 cells of 10,000 were treated with 100 ng/ml oligomycin without (OM-100) or with daily change of medium (OM-100 MC) for 5 days. The cells were counted by hemocytometer. Bars, S.D.; $n = 2$. B, during the 5-day growth, 20 μ l of medium was collected daily to measure glucose consumption (left panel) and lactate production (right panel). Bars, S.D.; $n = 2$. C, cell cycle analysis of H1299 after 72 h of growth without (top panel) or with oligomycin at 100 ng/ml (bottom panel). Both floating and adherent cells were collected and combined for the analysis. D, oligomycin dose-response growth curves in multiple cancer cells. E, the average of growth inhibition from oligomycin dosages at 1, 10, 100, and 1000 ng/ml were calculated and ranked. Bars, S.E., $n = 3$.

Treatment of H1650 cells with oligomycin demonstrated a similar shift of cells to the glycolysis-powered growth at a slower rate, but the growth inhibition by oligomycin was only 35%, corresponding to a smaller portion of OXPHOS in this cell line. We then compared the oligomycin dose-response curves among cancer cells and found a differential growth inhibition (Fig. 5D). Because almost all growth inhibition by oligomycin was shown at the dosages of 1000, 100, 10, and 1 ng/ml, we calculated the average of growth inhibition from these four dosages to represent the sensitivity and resistance of cancer cells to oligomycin (Fig. 5E). This sensitivity resistance profile is consistent with the prediction of OXPHOS dependence from the bioenergetic organizations of the cancer cells (Fig. 2D), demonstrating the specific OXPHOS suppression-related growth inhibition. Taken together, long term oligomycin treatment induces persistent energy stress in OXPHOS-dependent cells as indicated by growth inhibition, but cells survived by constantly accelerating glycolysis to maintain ATP homeostasis.

DISCUSSION

In this study, we have characterized the bioenergetic adaptation to the oligomycin-induced OXPHOS suppression in a group of cancer cells with heterogeneous respiration and glycolysis levels. We find that oligomycin at 100 ng/ml completely inhibits OXPHOS activity in ~1 h in cancer cells, regardless of the high or low original OXPHOS levels. Compared with hypoxia, oligomycin induces a significant level of glycolysis without activation of HIF-1 α and up-regulation of glycolytic enzyme expression. Therefore, the growth and survival of oligomycin-treated cells are different from the HIF-regulated hypoxia growth and survival, and OXPHOS suppression plays a major role in hypoxia-induced metabolism adjustment.

The study leads to the development of an oligomycin-based method to establish the bioenergetic organization in cancer cells, which accurately predicts the bioenergetic dependence of individual cancer cells on glycolysis and OXPHOS. The dependence on OXPHOS is studied here as the rise of signs of energy stress after oligomycin treatment, including glycolysis acceleration, ATP imbalance, AMPK activation, P-ACC induction, and cell growth inhibition. Not surprisingly, these signs of energy stress are detected at low levels or not at all in glycolysis-dependent U87MG, 786-0, and H838 cells.

H1299 cells, which depend on OXPHOS as well as aerobic glycolysis, experience slight ATP drops during the first 2 h of oligomycin treatment, suggesting that the stimulated glycolysis requires a catch-up to rebalance the fast loss of OXPHOS generated ATP in the beginning. After 2 h and beyond, H1299 cells under long term oligomycin treatment maintain this elevated level of glycolysis that sustains cellular ATP at the preoligomycin treatment levels, drives cell growth, and preserves cell survival. Nevertheless, even without ATP depletion, in OXPHOS-dependent cancer cells, the energy stress caused by the loss of OXPHOS ATP is maintained in the long term along with the presence of oligomycin. Inductions of P-ACC in H1299 cells are detected at 24 h of oligomycin treatment, and cell growth inhibition is induced proportional to cell dependence on OXPHOS.

The energy stress marker AMPK is known to be activated by ATP imbalance to induce P-ACC, stimulate glycolysis, and

inhibit cell growth. Although capable of performing the master regulatory role, our data point to a limited role of AMPK in regulating oligomycin-induced bioenergetic adaptation. First, AMPK is activated transiently, only during the 1–2 h of oligomycin treatment as cells are urgently replacing the loss of OXPHOS ATP with glycolysis ATP and experiencing a temporary ATP drop. After this power production switch is completed, AMPK activation recedes and is not detected at 3, 6, and 24 h of oligomycin treatment. Because cellular ATP is maintained after AMPK activation is completed, it can be ruled out that transient AMPK activation results from cellular ATP depletion as the result of cell death (22). In addition, we find that AMPK activation is not detected at all in *LKB1*-null A549 and H838 cells under energy stress induced by various means. One possibility is that the low level of AMPK activation, which cannot be reliably detected by P-AMPK on immunoblots, is sufficient to perform its physiological role. Another possibility is that there is an unknown master mechanism that performs a similar role that is capable of regulating glycolysis stimulation, P-ACC induction, and growth slowdown in the long term. This mechanism may depend on the initial AMPK activation to sense cellular energy imbalance or be directly activated by the imbalance.

Our findings that cancer cells can survive a complete OXPHOS suppression by readily replacing the OXPHOS-produced ATP with the inefficient glycolysis support the hypothesis that some level of Warburg effect originates from the OXPHOS defects. During this switch, cancer cells only experience some growth slowdown, which, according to cell cycle analysis, does not arrest cells at particular phases and does not accompany significant cell death. Therefore, it seems that OXPHOS ATP is not essential for growth and survival of cancer cells. Such a dispensability of the OXPHOS ATP may provide cancer cells opportunities to accumulate OXPHOS defects without detrimental impacts. The cell growth slowdown incurred from OXPHOS inhibition is a protective strategy for cancer cells during energy stresses, which can be overcome by further increasing glycolysis ATP during tumor evolution to reach a new bioenergetic homeostasis under the newly established bioenergetic organization. Once removed from the energy stress checkpoint, the more glycolytic and less OXPHOS tumors will gain growth advantage by being less sensitive to hypoxia stress. Because ROS-generating OXPHOS defects can also promote tumor malignancy (11, 12), it seems advantageous for cancer cells to accumulate certain OXPHOS defects and consequently drive up the Warburg effect. In addition, the heterogeneous bioenergetic organizations we characterized in this study display a continuous spectrum of shift to increasing glycolysis, which may represent a living snapshot of the dynamics of losing mitochondrial OXPHOS occurred *in vivo* during tumorigenesis.

REFERENCES

1. Warburg, O. (1956) *Science* **123**, 309–314
2. DeBerardinis, R. J., Lum, J. J., Hatzivassiliou, G., and Thompson, C. B. (2008) *Cell Metab.* **7**, 11–20
3. Kroemer, G., and Pouyssegur, J. (2008) *Cancer Cell* **13**, 472–482
4. Capuano, F., Guerrieri, F., and Papa, S. (1997) *J. Bioenerg. Biomembr.* **29**, 379–384

Adaptation to Oligomycin-induced OXPHOS Inhibition

- Cuezva, J. M., Krajewska, M., de Heredia, M. L., Krajewski, S., Santamaría, G., Kim, H., Zapata, J. M., Marusawa, H., Chamorro, M., and Reed, J. C. (2002) *Cancer Res.* **62**, 6674–6681
- Wallace, D. C. (2005) *Annu Rev. Genet.* **39**, 359–407
- Matoba, S., Kang, J. G., Patino, W. D., Wragg, A., Boehm, M., Gavrilova, O., Hurley, P. J., Bunz, F., and Hwang, P. M. (2006) *Science* **312**, 1650–1653
- López-Ríos, F., Sánchez-Aragó, M., García-García, E., Ortega, A. D., Berrendero, J. R., Pozo-Rodríguez, F., López-Encuentra, A., Ballestín, C., and Cuezva, J. M. (2007) *Cancer Res.* **67**, 9013–9017
- Samudio, I., Fiegl, M., McQueen, T., Clise-Dwyer, K., and Andreeff, M. (2008) *Cancer Res.* **68**, 5198–5205
- Gatenby, R. A., and Gillies, R. J. (2004) *Nat. Rev. Cancer* **4**, 891–899
- Petros, J. A., Baumann, A. K., Ruiz-Pesini, E., Amin, M. B., Sun, C. Q., Hall, J., Lim, S., Issa, M. M., Flanders, W. D., Hosseini, S. H., Marshall, F. F., and Wallace, D. C. (2005) *Proc. Natl. Acad. Sci. U.S.A.* **102**, 719–724
- Ishikawa, K., Takenaga, K., Akimoto, M., Koshikawa, N., Yamaguchi, A., Imanishi, H., Nakada, K., Honma, Y., and Hayashi, J. (2008) *Science* **320**, 661–664
- Hardie, D. G., Scott, J. W., Pan, D. A., and Hudson, E. R. (2003) *FEBS Lett.* **546**, 113–120
- Kahn, B. B., Alquier, T., Carling, D., and Hardie, D. G. (2005) *Cell Metab.* **1**, 15–25
- Kurth-Kraczek, E. J., Hirshman, M. F., Goodyear, L. J., and Winder, W. W. (1999) *Diabetes* **48**, 1667–1671
- Russell, R. R., 3rd, Bergeron, R., Shulman, G. I., and Young, L. H. (1999) *Am. J. Physiol.* **277**, H643–H649
- Marsin, A. S., Bertrand, L., Rider, M. H., Deprez, J., Beauloye, C., Vincent, M. F., Van den Berghe, G., Carling, D., and Hue, L. (2000) *Curr. Biol.* **10**, 1247–1255
- Marsin, A. S., Bouzin, C., Bertrand, L., and Hue, L. (2002) *J. Biol. Chem.* **277**, 30778–30783
- Almeida, A., Moncada, S., and Bolaños, J. P. (2004) *Nat. Cell Biol.* **6**, 45–51
- Almeida, A., Almeida, J., Bolaños, J. P., and Moncada, S. (2001) *Proc. Natl. Acad. Sci. U.S.A.* **98**, 15294–15299
- Motoshima, H., Goldstein, B. J., Igata, M., and Araki, E. (2006) *J. Physiol.* **574**, 63–71
- Hardie, D. G. (2000) *Curr. Biol.* **10**, R757–759
- Zhou, G., Myers, R., Li, Y., Chen, Y., Shen, X., Fenyk-Melody, J., Wu, M., Ventre, J., Doebber, T., Fujii, N., Musi, N., Hirshman, M. F., Goodyear, L. J., and Moller, D. E. (2001) *J. Clin. Invest.* **108**, 1167–1174
- Semenza, G. L. (2009) *Semin. Cancer Biol.* **19**, 12–16